J Inherit Metab Dis
DOI 10.1007/s10545-012-9526-6

ORIGINAL ARTICLE

Two neonatal cholestasis patients with mutations in the *SRD5B1* (*AKR1D1*) gene: diagnosis and bile acid profiles during chenodeoxycholic acid treatment

Yoshitaka Seki · Tatsuki Mizuochi · Akihiko Kimura · Tomoyuki Takahashi · Akira Ohtake · Shin-Ichi Hayashi · Toshiya Morimura · Yasuharu Ohno · Takayuki Hoshina · Kenji Ihara · Hajime Takei · Hiroshi Nittono · Takao Kurosawa · Keiko Homma · Tomonobu Hasegawa · Toyojiro Matsuishi

Received: 19 October 2011 / Revised: 19 July 2012 / Accepted: 25 July 2012

Abstract
Background and aims In two Japanese infants with neonatal cholestasis, 3-oxo-Δ^4-steroid 5β-reductase deficiency was diagnosed based on mutations of the *SRD5B1* gene. Unusual bile acids such as elevated 3-oxo-Δ^4 bile acids were detected in their serum and urine by gas chromatography–mass spectrometry. We studied effects of oral chenodeoxycholic acid treatment.
Patients and methods *SRD5B1* gene analysis used peripheral lymphocyte genomic DNA. Diagnosis and treatment of these two patients were investigated retrospectively and prospectively investigated.
Results With respect to *SRD5B1*, one patient was heterozygous (R266Q, a novel mutation) while the other was a compound heterozygote (G223E/R261C). Chenodeoxycholic acid treatment was effective in improving liver function and decreasing unusual bile acids such as 7α-hydroxy- and 7α,12α-dihydroxy-3-oxo-4-cholen-24-oic acids in serum and urine.

Communicated by: Peter Theodore Clayton

Y. Seki · T. Mizuochi · A. Kimura (✉) · T. Takahashi · T. Matsuishi
Department of Pediatrics and Child Health,
Kurume University School of Medicine,
67 Asahi-machi,
Kurume-shi 830-0011, Japan
e-mail: hirof@med.kurume-u.ac.jp

T. Takahashi
Division of Gene Therapy and Regenerative Medicine,
Cognitive and Molecular Research Institute of Brain Disease,
Kurume University,
Kurume, Japan

A. Ohtake
Department of Pediatrics, Faculty of Medicine,
Saitama Medical University,
Saitama, Japan

S.-I. Hayashi · T. Morimura · Y. Ohno
Department of Pediatric Surgery, Faculty of Medicine,
Saitama Medical University,
Saitama, Japan

T. Hoshina · K. Ihara
Department of Pediatrics, Graduate School of Medical Sciences,
Kyushu University,
Fukuoka, Japan

H. Takei · H. Nittono
Institution of Bile Acid, Junshin Clinic,
Tokyo, Japan

T. Kurosawa
Faculty of Pharmaceutical Sciences,
Health Sciences University of Hokkaido,
Hokkaido, Japan

K. Homma
Central clinical Laboratories, Keio University Hospital,
Tokyo, Japan

T. Hasegawa
Department of Pediatrics, Keio University School of Medicine,
Tokyo, Japan

Published online: 16 November 2012

Conclusion Primary bile acid treatment using chenodeoxycholic acid was effective for these patients treated in early infancy before the late stage of chronic cholestatic liver dysfunction.

Abbreviations

5β-reductase	3-oxo-Δ^4-steroid 5β-reductase
TBA	total bile acids
GGT	γ-glutamyltransferase
3β-HSD	3β-hydroxy-Δ^5-C_{27}-steroid dehydrogenase/isomerase
ALT	alanine aminotransferase
GC-MS	gas chromatography–mass spectrometry
CDCA	chenodeoxycholic acid
AST	aspartate aminotransferase
UDCA	ursodeoxycholic acid
Cr	creatinine
CMV	cytomegalovirus
CA	cholic acid

Introduction

In 1988, Clayton et al reported that in pediatric patients with severe liver disease such as cholestatic disease with cirrhosis and fumarylactoacetase deficiency, the major unusual bile acids detected were 3-oxo-Δ^4 bile acids, such as 7α-hydroxy- and 7α,12α-dihydroxy-3-oxo-4-cholen-24-oic acids. These patients had secondary 3-oxo-Δ^4-steroid 5β-reductase (5β-reductase) deficiency. At about the same time, primary 5β-reductase deficiency was described (Setchell et al 1988). This inborn error of bile acid synthesis is very rare and shows autosomal recessive inheritance. Main findings in 5β-reductase deficiency are normal or slightly elevated concentrations of total bile acids (TBA) and γ-glutamyltransferase (GGT) in serum; elevated conjugated bilirubin and alanine aminotransferase (ALT); and fatty stools. During synthesis of bile acids from cholesterol in the classic pathway, decreased activity of 5β-reductase enzymes reduces synthesis of primary bile acids and increases synthesis of 3-oxo-Δ^4 bile and allobile acids. However, no analysis of the 5β-reductase gene was reported in Setchell's patient.

The most common inborn error of bile acid synthesis is 3β-hydroxy-Δ^5-C_{27}-steroid dehydrogenase/isomerase (3β-HSD) deficiency, which has a clinical presentation similar to that of 5β-reductase deficiency: neonatal cholestatic jaundice, elevated transaminases but normal GGT, and evidence of fat-soluble vitamin malabsorption (Subramaniam et al 2010). Moreover, 3-oxo-Δ^4 bile acids can be detected as major urinary bile acids in primary 5β-reductase deficiency and secondary deficiency, such as in neonatal hemochromatosis (Sumazaki et al 1997; Lemonde et al 2003; Ueki et al 2009; Clayton 2011).

Lemonde et al (2003) and Gonzales et al (2004) reported *SRD5B1* (*AKR1D1*) gene analysis in 5β-reductase deficiency involving chromosome 7q32-33. In these two reports describing five patients, mutations in the *SRD5B1* gene were identified in all, including three homozygous mutations and two compound heterozygous mutations. Recently we reported two heterozygous mutations in patients diagnosed with 5β-reductase deficiency by bile acid analysis using gas chromatography–mass spectrometry (GC-MS) (Ueki et al 2009).

Here we report two Japanese infants, a 6-month-old boy, and a 9-month-old girl, with 5β-reductase deficiency resulting from a heterozygous mutation of *SRD5B1* in one and compound heterozygous mutations of the same gene in the other. We examined the clinical effect of oral chenodeoxycholic acid (CDCA) treatment in these two patients.

Patients and methods

Patient report

Patient 1 A male Japanese infant was delivered at 37 weeks gestational age after an uneventful pregnancy. His parents were not consanguineous and were healthy, without liver disease. At birth, he showed abdominal distension and metabolic acidosis. Abdominal radiography and computed tomography disclosed free air. We performed exploratory laparotomy at Saitama Medical University Hospital at 2 days after birth for suspected gastrointestinal perforation. We intraoperatively diagnosed the patient with meconium peritonitis from jejunal perforation associated with neonatal intussusception.

He soon developed jaundice, which was present until 6 months of age. We carried out technetium-99 m (^{99m}Tc)-DISIDA cholescintigraphy at 2 months and liver biopsy at 3 months. Cholescintigraphy failed to show intestinal radioactivity, while liver microscopic findings included giant cell transformation and wide fibrotic bands at portal areas (Fig. 1).

Laboratory results included serum aspartate aminotransferase (AST) concentration of 344 U/L (normal, <37); ALT, 441 I/L (<31); and total/direct bilirubin, 4.4/3.4 mg/dL (<1.2/0.4). GGT concentration in serum was 46 U/L (<52). We did not examine serum TBA at admission, but when we suspected an inborn error of bile acid synthesis from the results above, we analyzed serum and urine bile acids using GC-MS (Table 1). Results of the bile acid analysis suggested 5β-reductase deficiency, and the patient was given ursodeoxycholic acid (UDCA) treatment.

Patient 2 A female Japanese infant with a birth weight of 2832 g was delivered without complications by spontaneous vaginal delivery at a gestational age of 38 weeks after an

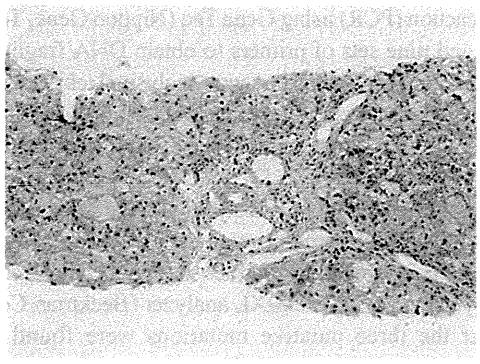

Fig. 1 Liver pathologic findings of patient 1. A liver biopsy specimen from patient 1 at 3 months showed lobular disarray resulting from extensive giant cell transformation and wide fibrotic bands in portal areas (Azan stain; magnification, x100)

uneventful pregnancy, her mother's first. The parents were not consanguineous and were healthy, without liver disease.

Progressive jaundice became apparent in the infant at 3 months. At 6 months, the patient was referred to Kyushu University Hospital because of jaundice and liver dysfunction.

On physical examination, growth and development were within the normal range. No dysmorphic features were present. Hepatomegaly and jaundice were noted. Neurologic findings were normal. Stools were gray. Initial laboratory results included serum concentrations of AST, 315 U/L; ALT, 229 U/L; alkaline phosphatase, 2,717 U/L (115 to 359); total/direct bilirubin, 6.3/3.6 mg/dL; albumin, 4.8 g/dL (4.0 to 5.0); total cholesterol, 216 mg/dL (128 to 219); prothrombin time, 14.8 s (10.0 to 13.5); and blood ammonia, 66 μg/dL (<66). Serum GGT was 61 U/L and serum TBA, 5.2 μmol/L (<10). Other causes of liver disease such as autoimmune hepatitis, chronic viral hepatitis, and other metabolic conditions were excluded by appropriate investigations. Abdominal ultrasonography showed a visible gallbladder and hepatomegaly; no choledochal cyst, bile duct dilation, or ascites was demonstrated. Serial technetium-99 m (^{99m}Tc)-DISIDA cholescintigraphy indicated that tracer entered the intestine. We suspected an inborn error of bile acid synthesis from the results above and analyzed serum and urine bile acids by GC-MS at 9 months of age (Table 1). Based on results of bile acid analysis, we suspected 5β-reductase deficiency.

Table 1 Bile acid analysis using gas chromatography-mass spectroscopy in two patients with 3-oxo-Δ^4-steroid 5β-reductase deficiency

	Patient 1 (6 months old)	Patient 2 (9 months old)	Infants with cholestasis[a] (n=2)	Normal infants[b] (n=4)
Serum (μmol/L)				
Cholic acid	n.d.	n.d.	200.1–209.7	0.2–1.8
Chenodeoxycholic acid	0.1	n.d.	55.1–56.8	1.2–5.3
Deoxycholic acid	0.2	n.d.	n.d.	n.d.
Lithocholic acid	n.d.	n.d.	n.d.	n.d.
Ursodeoxycholic acid	1.5	n.d.	0.5–8.6	n.d.
Allo-cholic acid	n.d.	n.d.	0.2–0.8	n.d.
Allo-chenodeoxycholic acid	0.9	n.d.	n.d.	n.d.
7α,12α-Dihydroxy-3-oxo-4-cholen-24-oic acid	0.3	14.4	n.d.–3.3	n.d.
7α-Hydroxy-3-oxo-4-cholen-24-oic acid	1.7	10.7	n.d.	n.d.
Others	0.6	2.3	6.6–1.1	n.d.–0.9
Total bile acids	5.3	27.4	265.1–277.7	1.4–6.2
Urine (μmol/mmol Cr)				
Cholic acid	0.2	n.d.	10.1–29.4	0.03–0.3
Chenodeoxycholic acid	n.d.	n.d.	1.0–18.1	0.01–0.1
Deoxycholic acid	0.1	n.d.	n.d.–0.2	n.d.–0.02
Lithocholic acid	n.d.	n.d.	n.d.–0.1	n.d.
Ursodeoxycholic acid	0.9	n.d.	0.1–17.4	n.d.–0.02
Allo-cholic acid	0.8	n.d.	0.1–0.3	n.d.–0.05
Allo-chenodeoxycholic acid	n.d.	n.d.	n.d.	n.d.
7α,12α-Dihydroxy-3-oxo-4-cholen-24-oic acid	121.1	37.5	10.2–27.1	n.d.
7α-Hydroxy-3-oxo-4-cholen-24-oic acid	2.8	21.4	1.0–1.2	n.d.
Others	n.d.	0.2	3.0–23.4	0.04–2.2
Total bile acids	125.9	59.1	25.7–116.9	0.1–2.6

[a] progressive familial intrahepatic cholestasis type 1 (2 and 11 months old); [b] 2, 5, 6, and 9 months old

n.d. not detected

Hepatitis C virus antibody and hepatitis B virus s antigen in the two patients were not detected, and autoimmune hepatitis was ruled out by negative anti-nuclear antibody test results, immunoglobulin G (420 mg/dL), and, in patient, liver histologic findings. In patient 1, progressive familial intrahepatic cholestasis was ruled out by bile acid analysis using GC-MS.

Qualitative and quantitative bile acid analysis

Serum and urine samples were collected and stored at −25 °C until analysis. Concentrations of individual bile acids in the urine were corrected for creatinine (Cr) concentration and expressed as μmol/mmol of Cr.

After we synthesized certain specific unusual bile acids, such as 3β-hydroxy-Δ^5 (Tohma et al 1986), 3-oxo-Δ^4 (Leppik 1983) and allo-bile acids (Ueki et al 2009) frequently seen in inborn errors of bile acid synthesis, we routinely analyzed bile acids in patient urine and serum by GC-MS using selected ion monitoring of the characteristic fragments of the methyl ester-dimethylethylsilyl ether-methoxime derivatives of bile acids as described previously (Kimura et al 1999), after enzymatic hydrolysis (choloylglycine hydrolase 30 units) and solvolysis (sulfatase 150 units; Sigma Chemical, St. Louis, MO).

The two patients in this study had bile acids in serum and urine analyzed using GC-MS on admission and during bile acid treatment.

Liver functional tests, bile acid analysis, and urinary steroid analysis before and after CDCA treatment suspension

After informed consent, we stopped CDCA treatment for 1 month in patient 1. We examined AST, ALT, serum and urinary bile acids, as well as urinary steroids, before and during the CDCA treatment suspension. We measured 5α- and 5β- metabolites of both cortisol and cortisone, such as tetrahydrometabolites including THFs (5α-tetrahydrocortisol, 5β-tetrahydrocortisol) and THEs (5α-tetrahydrocortisone, 5β-tetrahydrocortisone) by GC-MS using selected ion monitoring (Homma et al 2003).

In patient 2, we could not obtain consent for CDCA treatment suspension from the patient's parents. We did examine urinary steroids during CDCA treatment.

Genetic analysis

With informed consent, *SRD5B1* gene analysis was performed using genomic DNA from peripheral lymphocytes from the two patients, their parents, and 50 healthy individuals. DNA fragments spanning the nine coding regions and exon-intron junctions of the *SRD5B1* gene were amplified by polymerase chain reaction (PCR) using Gene Taq (Nippon Gene, Toyama, Japan) and nine sets of primers to obtain DNA fragments of optimal length for direct sequence analysis (Ueki et al 2009).

After enzymatic processing with ExoSAP-IT (USB, Cleveland, OH), direct sequencing of amplified PCR products was carried out with a DTCS Quick Start Kit (Beckman Coulter, Fullerton, CA) according to the manufacturer's protocol, using the same primers as for PCR amplification. The sequencing reaction product was analyzed electrophoretically using an SEQ2000XL analyzer (Beckman Coulter).

After the three putative mutations were found in the patients, their parents and 50 healthy individuals were screened for these three mutations by direct sequence analysis.

All studies were undertaken with permission from the Ethical Committee of Kurume University School of Medicine.

Results

Biochemical identification of an inborn error of bile acid synthesis

Patient 1 had jaundice since the early neonatal period, especially after surgery. Patient condition stabilized with UDCA (7.5 mg/kg/day) treatment. UDCA treatment was effective against liver dysfunction, such as elevated ALT and total bilirubin. After diagnosis, we added CDCA (5 mg/kg/day) to UDCA treatment. Liver dysfunction resolved completely with combined UDCA (7.5 mg/kg/day) and CDCA (5 mg/kg/day) treatment (Fig. 2a). Serum total bilirubin concentration decreased to the normal range, followed by a decrease in ALT. While concentrations of 3-oxo-Δ^4 bile acids in serum and urine were not reduced by UDCA (7.5 mg/kg/day) treatment, combined UDCA (7.5 mg/kg/day) and CDCA (5 mg/kg/day) treatment, gradually decreased serum 3-oxo-Δ^4 bile acids to undetectable amounts (less than 1 μmol/L). Urinary 3-oxo-Δ^4 bile acids decreased after serum fluctuation. Since UDCA treatment was stopped at 14 months of age, liver function and bile acid profiles in serum and urine have been stable with CDCA (5 mg/kg/day) monotherapy.

Importantly, during CDCA treatment suspension for 1 month, values for total/direct bilirubin, AST, and ALT remained in the normal ranges (Table 2).

Fig. 2 Clinical course of patient 1 (**a**) and patient 2 (**b**). Responses of ▶ serum alanine aminotransferase (ALT; *filled circles*), total bilirubin (T Bil; *open circles*), serum total bile acids (s-TBA; *filled squares*), serum 3-oxo-Δ^4 bile acids (s-3-oxo-Δ^4; *open squares*), urine total bile acids (u-TBA; *filled triangles*), and urine 3-oxo-Δ^4 bile acids (u-3-oxo-Δ^4; *open triangles*) to treatment with combined ursodeoxycholic acid (UDCA) and chenodeoxycholic acid (CDCA) treatment or CDCA mono-treatment are shown

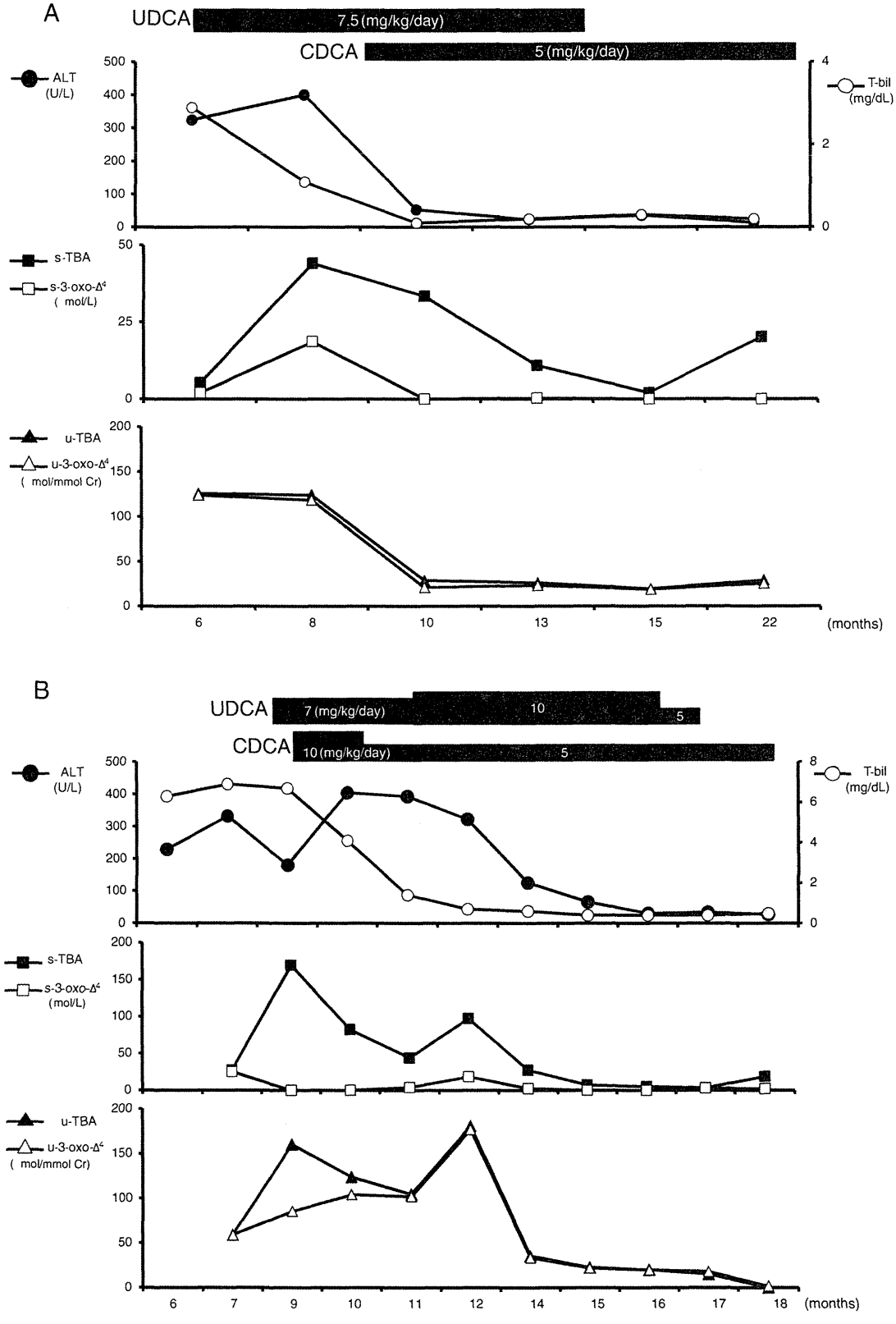
A
UDCA
7.5 (mg/kg/day)
CDCA
5 (mg/kg/day)
ALT (U/L)
T-bil (mg/dL)
s-TBA
s-3-oxo-Δ4 (mol/L)
u-TBA
u-3-oxo-Δ4 (mol/mmol Cr)
(months)
B
UDCA
7 (mg/kg/day)
10
5
CDCA
10 (mg/kg/day)
5
ALT (U/L)
T-bil (mg/dL)
s-TBA
s-3-oxo-Δ4 (mol/L)
u-TBA
u-3-oxo-Δ4 (mol/mmol Cr)
(months)

Table 2 Liver function tests and bile acid analysis in patient 1 before and during CDCA treatment suspension

	Before CDCA treatment suspension	During CDCA treatment suspension	
		After 2 weeks	After 4 weeks
Total bilirubin (mg/dL)	0.2	0.2	0.3
Direct bilirubin (mg/dL)	0.1	0.1	0.1
AST (U/L)	29	29	28
ALT (U/L)	13	12	12
Serum (μmol/L)			
Usual bile acids	23.8	5.2	1.5
Allo-bile acids	1.1 (4.2 %)	1.6 (18.9 %)	1.4 (29.9 %)
3-Oxo Δ^4 bile acids	1.4 (5.2 %)	1.7 (19.7 %)	1.6 (34.3 %)
Other bile acids	0.1	0.1	0.1
Total bile acids	26.4	8.6	4.7
Urine (μmol/mmol Cr)			
Usual bile acids	1.73	0.51	0.24
Allo-bile acids	0.30	0.17	0.23
3-Oxo Δ^4 bile acids	37.08 (93.6 %)	30.58 (96.4)	33.66 (97.4 %)
Other bile acids	0.50	0.46	0.44
Total bile acids	39.62	31.72	34.57

AST aspartate aminotransferase, *ALT* alanine aminotransferase, *Usual bile acids* cholic acid + chenodeoxycholic acid + ursodeoxycholic acid + deoxycholic acid + lithocholic acid; Allo-bile acids, allo-cholic acid + allo-chenodeoxycholic acid, *3-Oxo Δ^4 bile acids* 7α,12α-Dihydroxy-3-oxo-4-cholen-24-oic acid + 7α-Hydroxy-3-oxo-4-cholen-24-oic acid

Patient 2 began UDCA (7 mg/kg/day) treatment at 8 months of age without improvement of clinical symptoms or liver function. After diagnosis, we added CDCA (10 mg/kg/day) to UDCA treatment at 9 months of age. Liver dysfunction, ALT and serum TBA increased, but 3-oxo-Δ^4 bile acids in serum decreased. Nearly all serum TBA was CDCA, while concentrations of TBA and 3-oxo-Δ^4 bile acids in urine were increased (Fig. 2b). We then decreased the dose of CDCA from 10 to 5 mg/kg/day and increased the dose of UDCA from 7 to 10 mg/kg/day. This treatment was effective against liver dysfunction. Serum concentrations of total bilirubin decreased to the normal range, followed by a decrease in ALT as occurred with patient 1. Concentrations of TBA and 3-oxo-Δ^4 bile acids in serum and urine gradually decreased. Clinical course, liver function parameters, and bile acid profiles in serum and urine gradually improved with CDCA monotherapy at 17 months of age. When serum ALT and TBA in serum and urine became elevated, we detected elevated serum titers of anti-cytomegalovirus (CMV) antibodies (IgM normal, under 0.34 at 6 months of age; but rising to 1.27 at 11 months). Serum IgG antibodies at 6 months of age were under 2.0 (normal), rising to 28.0 at 11 months.

We could not find evidence of liver cirrhosis such as splenomegaly or prominent abdominal veins in either patient during this study.

Results of serum and urinary bile acid analysis and urinary steroid analysis before and during CDCA treatment suspension for 1 month

In patient 1, the main usual bile acid in serum was CDCA during CDCA treatment. During CDCA treatment suspension for 1 month, small amounts of allo- and ketonic bile acids were detected in serum, as at the time of initiation of CDCA treatment. As the month continued, however, percentages of allo- and ketonic bile acids among total bile acids gradually increased from 4.2 and 5.2 % to 29.9 and 34.3 %, respectively (Table 2). On the other hand, values and percentages of allo- and ketonic bile acids in urine did not change from those present during CDCA treatment.

In the two patients, excretion of 5β metabolites, such as 5β-tetrahydrocortisol and 5β-tetrahydrocortisone, was sharply reduced (Table 3). Overall alteration in cortisol and cortisone metabolism was evident from high 5α/5β ratios (Table 3).

Identification of *SRD5B1* gene defects

We identified one previously unreported mutation in one patient and two previously reported mutations in the other.

Patient 1 A single novel heterozygous mutation was found in exon 7, at nucleotide number 866, representing a G-to-A substitution causing an amino acid change from arginine at position 266 to glutamine (R266Q). The mutation was detected in heterozygous form in the patient's mother, but was absent in the father and controls.

Patient 2 Two previously reported heterozygous mutations were found. One was detected in exon 6, at nucleotide number 737, representing a G-to-A substitution causing an amino acid change from glycine at position 223 to glutamic acid (G223E). G223E was detected in heterozygous form in the patient's father, but was absent in the mother and 50 healthy individuals. The other mutation was detected in exon 7, at nucleotide number 850, representing a C-to-T substitution causing an amino acid change from arginine at position 261 to cysteine (R261C). R261C was detected in heterozygous form in the patient's mother, but was absent in the father and controls.

The above nucleotide numbers indicating positions of individual mutations are based on GenBank accession no. NM_0059892.

Table 3 Urinary steroid analysis in patient 1 during CDCA treatment and CDCA treatment suspension, and in patient 2 during CDCA treatment

Patient 1 (3 years of age, male)			
	During CDCA treatment	During CDCA treatment suspension (after 4 weeks)	Normal range*
5αTHF (mg/g Cr)	1.62	1.08	0.95–3.97
5βTHF (mg/g Cr)	0.01	<0.01	0.91–4.41
5αTHE (mg/g Cr)	0.37	0.19	0.12–0.53
5βTHE (mg/g Cr)	0.03	0.02	1.61–6.36
5α/5βTHF	231	270	0.79–2.31
5α/5βTHE	12.4	8.07	0.05–0.18
Patient 2 (2 years of age, female)			
	During CDCA treatment	Normal range**	
5αTHF (mg/g Cr)	2.86	1.04–2.35	
5βTHF (mg/g Cr)	0.03	0.97–1.65	
5αTHE (mg/g Cr)	0.39	0.11–0.30	
5βTHE (mg/g Cr)	0.18	2.32–5.88	
5α/5βTHF	110	1.04–1.70	
5α/5βTHE	2.14	0.04–0.07	

THF tetrahydrocortisol, *THE* tetrahydrocortisone

*normal range, from 2 to 4 years old, male, $n=10$, 24-h urine samples, 2.5–97.5th percentile

**normal range, from 2 to 4 years old, female, $n=10$, 24-h urine samples, 2.5–97.5th percentile

Discussion

In our two patients with 5β-reductase deficiency and *SRD5B1* mutation, CDCA treatment was effective in improving liver function and reducing unsaturated ketonic bile acids in serum and urine. Oral bile acid treatment such as cholic acid (CA) is safe and effective for treating most common inborn errors of bile acid synthesis, including 5β-reductase deficiency (Gonzales et al 2009). CA treatment may be superior to alternatives because CA activates negative feedback regulation of bile acid synthesis to inhibit production of hepatotoxic metabolites more effectively than CDCA, and is not itself hepatotoxic. However, CA is not available for clinical use in Japan. In a previous report (Clayton et al 1996), combined CA and CDCA were used together to treat 5β-reductase deficiency. We found that oral bile acid treatment using CDCA monotherapy could be effective for patients with 5β-reductase deficiency. However, assessment of CDCA monotherapy ultimately may require longer follow-up.

In bile acid analysis results during combined UDCA and CDCA treatment, exogenous UDCA was detected more in urine than in serum, while exogenous CDCA was detected more in serum than in urine (data not shown). We believe that after transport from hepatocyte to blood by hepatic multidrug resistance-related protein (MRP) 4 in the hepatocytic basolateral membrane, hydrophilic UDCA may undergo preferential renal excretion mediated by renal MRP 4 (Wagner and Trauner 2005; Marschall et al 2005; Stapelbroek et al 2010). Unsaturated ketonic bile acids – 3-oxo-Δ^4 bile acids – were detected more in urine than in serum; these are transported across the basolateral membrane into the blood via MRP3 (Yamaguchi et al 2010). Then 3-oxo-Δ^4 bile acids are excreted directly into urine by a bile acid transporter. As a result, increased urinary 3-oxo-Δ^4 bile acids may be detected in this disease.

Even with normal liver function, we detected 3-oxo-Δ^4 bile acids in serum and especially in urine. We speculate that the negative feedback induced by 5 mg/kg/day of CDCA may be incomplete, but liver function might worsen from a higher CDCA dose. A CDCA dose such as 10 mg/kg/day may provide very effective negative feedback at cholesterol 7α-hydroxylase via the farnesoid X receptor (Gonzales et al 2009). Patients so treated require close follow-up. Liver function tests, analysis of bile acids in serum and urine, determination of fibrosis markers such as type IV collagen 7 s domain, and especially liver biopsy are desirable. However, changes in urinary 3-oxo-Δ^4 bile acids may not always indicate stage of disease; since we analyze bile acids using single serum and urine specimens, we cannot eliminate diet-related variability. Moreover, some liver diseases reduce activity of 5β-reductase, including metabolic disorders, viral infections (Clayton et al 1988; Kimura et al 1998), and drug-induced hepatitis. Therefore, neonatal viral infections such as CMV infection as well as medication effects must be considered. We suspected that 3-oxo-Δ^4 bile acids in serum and urine from our patient 2 were increased by intrinsic hepatotoxicity of CDCA (Fig. 2b) and/or effects of CMV hepatitis.

In our patients with 5β-reductase deficiency, time needed to normalize laboratory data during oral bile acid treatment using combined UDCA and CDCA treatment or CDCA monotherapy has been longer than for patients with 3β-HSD deficiency (Yamato et al 2001; Mizuochi et al 2010). We recommended that patients with 5β-reductase deficiency begin oral bile acid treatment in early infancy, before

deficiency causes chronic cholestatic liver dysfunction by as early as 10 months (Gonzales et al 2004; Ueki et al 2009).

In patient 1, results of serum liver function tests such as total bilirubin and ALT did not change during or after CDCA treatment suspension, but percentages of allo- and ketonic bile acids among total bile acids in serum gradually increased (Table 2). Also, patients 1 and 2 showed sharply reduced production of the 5β metabolites 5β-tetrahydrocortisol and 5β-tetrahydrocortisone (Table 3), as reported by Palermo et al (2008). Therefore, we believe that patient 1, with a heterozygous mutation, had a 5β-reductase deficiency. Like deficient patients reported by Palermo et al (2008) and Ueki et al (2009), our patient 1 showed no change in liver function, even though results of bile acid analysis in serum and urine when CDCA was suspended were the same as those at diagnosis of 5β-reductase deficiency. The basis of this pathophysiologic state is unknown, but alleviation of cholestatic liver disease by early primary bile acid administration appeared to preserve liver function. We suspect that activity of hepatocytic MRP3 may be low during early infancy, permitting cholestatic liver disease to arise from hepatocytic accumulation of unsaturated ketonic bile acids such as 3-oxo-Δ^4 bile acids in hepatocytes. With maturation, activity of hepatocytic MRP3 normally increases, favoring transport of 3-oxo-Δ^4 bile acids across the basolateral membrane into the blood (Yamaguchi et al 2010) and ultimately the urine—presumably avoiding late-infancy liver damage.

The human *SRD5B1* gene contains nine coding exons corresponding to 326 amino acids; so far, seven distinct mutations causing 5β-reductase deficiency have been reported (Lemonde et al 2003; Gonzales et al 2004; Ueki et al 2009). Transmission of this deficiency is considered autosomal recessive. Here we describe genetic analysis of the *SRD5B1* gene in two patients with 5β-reductase deficiency, identifying one new mutation (R266Q) and two previously reported mutations (G223E and R261C) (Gonzales et al 2004; Ueki et al 2009; Drury et al 2010). Screening for R266Q was undertaken in 50 healthy individuals, proving absent in all. Moreover, an adverse effect from the mutation was predicted by Polymorphism Phenotyping software (version 2; Adzhubei et al 2010; score, 0.995). We believe that the heterozygous R266Q mutation likely contributed to loss of 5β-reductase function in patient 1, although we still suspect that he may have an unknown mutation in another allele—making him a compound heterozygote. Unfortunately we could not determine expression of 5β-reductase protein in patient 1 because no frozen liver sample had not been retained. Patient 2 had two heterozygous mutations (G223E/R261C), receiving one G223E mutation from each parents making her a compound heterozygote for the *SRD5B1* gene.

In conclusion, we diagnosed two patients with 5β-reductase deficiency, one with heterozygous and the other with compound heterozygous mutation in the *SRD5B1* gene. Primary bile acid treatment in early infancy using CDCA (5 mg/kg/day) proved effective in both of these patients.

Conflict of interest None.

References

Adzhubei IA, Schmidt S, Peshkin L et al (2010) A method and server for predicting damaging missense mutations. Nat Methods 7:248–249

Clayton PT (2011) Disorders of bile acid synthesis. J Inherit Metab Dis 34:593–604

Clayton PT, Patel E, Lawson AM et al (1988) 3-Oxo-Δ^4 bile acids in liver disease. Lancet 1:1283–1284

Clayton PT, Mills KA, Johnson AW, Barabino A, Marazzi MG (1996) Δ^4-3-Oxosteroid 5β-reductase deficiency: failure of ursodeoxycholic acid treatment and response to chenodeoxycholic acid plus cholic acid. Gut 38:623–628

Drury JE, Mindnich R, Penning TM (2010) Characterization of disease-related 5β-reductase (AKR1D1) mutations reveals their potential to cause bile acid deficiency. J Biol Chem 285:24529–24537

Gonzales E, Cresteil D, Baussan C, Dabadie A, Gerhardt M-F, Jacquemin E (2004) SRD5B1 (AKR1D1) gene analysis in Δ^4-3-oxosteroid 5β-reductase deficiency: evidence for primary genetic defect. J Hepatol 40:716–718

Gonzales E, Gerhardt MF, Fabre M et al (2009) Oral cholic acid for hereditary defects of primary bile acid synthesis: a safe and effective long-term therapy. Gastroenterology 137:1310–1320

Homma K, Hasegawa T, Masumoto M et al (2003) Reference values for urinary steroids in Japanese newborn infants: gas chromatography/mass spectrometry in selected ion monitoring. Endocr J 50:783–792

Kimura A, Suzuki M, Murai T et al (1998) Urinary 7α-hydroxy-3-oxochol-4-en 24-oic and 3-oxochola-4,6-dien-24-oic acids in infants with cholestasis. J Hepatol 28:270–279

Kimura A, Mahara R, Inoue T et al (1999) Profile of urinary bile acids in infants and children: developmental pattern of excretion of unsaturated ketonic bile acids and 7β-hydroxylated bile acids. Pediatr Res 45:603–609

Lemonde HA, Custard EJ, Bouquet J, Duran M, Scambler PJ, Clayton PT (2003) Mutation in *SRD5B1* (*AKR1D1*), the gene encoding Δ^4-3-oxosteroid 5β-reductase, in hepatitis and liver failure in infancy. Gut 52:1494–1499

Leppik RA (1983) Improved synthesis of 3-keto, 4-ene-3keto-, and 4,6-diene-3-keto bile acids. Steroids 41:475–484

Marschall H-U, Wagner M, Zollner G et al (2005) Complementary stimulation of hepatobiliary transport and detoxification systems by rifampicin and ursodeoxycholic acid in humans. Gastroenterology 129:476–485

Mizuochi T, Kimura A, Ueki I et al (2010) Molecular genetic and bile acid profiles in two Japanese patients with 3β-hydroxy-Δ^5-C_{27}-steroid dehydrogenase/isomerase deficiency. Pediatr Res 68:258–263

Palermo M, Marazzi MG, Hughes BA, Stewart PM, Clayton PT, Shackleton CHL (2008) Human Δ^4-3-oxosteroid 5β-reductase (AKR1D1) deficiency and steroid metabolism. Steroids 73:417–423

Setchell KDR, Suchy FJ, Welsh MB, Zimmer-Nechemias L, Heubi J, Balistreri WF (1988) Δ^4-3-Oxosteroid 5β-reductase deficiency described in identical twins with neonatal hepatitis. J Clin Invest 82:2148–2157

Stapelbroek JM, von Erpecum KJ, Klomp LWJ, Houwen RHJ (2010) Liver disease associated with canalicular transport defects: current and future therapies. J Hepatol 52:258–271

Subramaniam P, Clayton PT, Portmann BC, Mieli-Vergani G, Hadzid N (2010) Variable clinical spectrum of the most common inborn error of bile acid metabolism-3β-hydroxy-Δ^5-C_{27}-steroid dehydrogenase deficiency. J Pediatr Gastroenterol Nutr 50:61–66

Sumazaki R, Nakamura N, Shoda J, Kurosawa T, Tohma M (1997) Gene analysis in Δ^4-3-oxosteroid 5β-reductase deficiency. Lancet 349:329

Tohma M, Mahara R, Takeshita H, Kurosawa T (1986) A convenient synthesis of 3β,12α-, 3β,7α-, and 3β,7β-dihydroxy-5-cholen-24-oic acids: unusual bile acids in human biological fluids. Steroids 48:331–338

Ueki I, Kimura A, Chen H-L et al (2009) *SRD5B1* gene analysis needed for the accurate diagnosis of primary 3-oxo-Δ^4-steroid 5β-reductase deficiency. J Gastroenterol Hepatol 24:776–785

Wagner M, Trauner M (2005) Transcriptional regulation of hepatobiliary transport systems in health and disease: implications for a rationale approach to the treatment of intrahepatic cholestasis. Ann Hepatol 4:77–99

Yamaguchi K, Murai T, Yabuuchi H, Kurosawa T (2010) Measurement of transport activities of bile acids in human multidrug resistance-associated protein 3 using liquid chromatography-tandem mass spectrometry. Anal Sci 26:317–323

Yamato Y, Kimura A, Murai T et al (2001) 3β-Hydroxy-Δ^5-C_{27}-steroid dehydrogenase deficiency: diagnosis and treatment. J Pediatr Child Health 37:516–519

Clinical Endocrinology (2012) 76, 78–87 doi: 10.1111/j.1365-2265.2011.04165.x

ORIGINAL ARTICLE

Identification of a novel mutation in the exon 2 splice donor site of the *POU1F1/PIT-1* gene in Japanese identical twins with mild combined pituitary hormone deficiency

Hiroshi Inoue*†, Tokuo Mukai‡, Yukiko Sakamoto†, Chizuko Kimura†, Natsumi Kangawa†, Mitsuo Itakura†, Tsutomu Ogata§, Yoshiya Ito‡ and Kenji Fujieda‡ on behalf of the Japan Growth Genome Consortium

*Diabetes Therapeutics and Research Center and †Division of Genetic Information, Institute for Genome Research, The University of Tokushima, Tokushima, ‡Department of Paediatrics, Asahikawa Medical University, Asahikawa and §Department of Endocrinology and Metabolism, National Research Institute for Child Health and Development, Tokyo, Japan

Summary

Context To date, approximately 35 different *POU1F1* mutations have been described in patients with familial and sporadic combined pituitary hormone deficiency (CPHD) from different ethnic backgrounds. The majority are missense mutations clustered within the conserved POU-specific and POU-homeo domains, encoded by exons 4 and 6, respectively.

Objectives This study aimed to identify the molecular basis and clinical characteristics of a Japanese CPHD family with a novel *POU1F1* mutation.

Design The *POU1F1* gene was sequenced in identical twin brothers with mild CPHD. The mutation identified was also evaluated in family members as well as 188 Japanese controls and then examined in functional studies.

Results A novel heterozygous splice site mutation (Ex2 + 1G>T; c.214 + 1G>T) was detected. This mutation was also present in their undiagnosed mother, but not in any of the controls. *In vitro* splicing studies suggested this mutation to result in an in-frame skipping of exon 2, thus producing an internally deleted protein lacking most of the R2 transactivation subdomain (TAD-R2). Heterologous expression studies of the mutated POU1F1 protein showed only modest reductions in its transactivation activities in HEK293T cells, while acting as a dominant-negative inhibitor of the endogenous activities of POU1F1 in pituitary GH3 cells.

Conclusions This is the first report of a mutation at the exon 2 donor splice site of *POU1F1*, affecting TAD-R2. The addition of this mutation to the growing list of pathological *POU1F1* mutations may provide deeper insights into clinical heterogeneity in the expressions of individual mutations and a better understanding of the structure–function relationships of POU1F1.

(Received 12 April 2011; returned for revision 10 May 2011; finally revised 28 June 2011; accepted 29 June 2011)

Correspondence: Hiroshi Inoue, Division of Genetic Information, Institute for Genome Research, The University of Tokushima, Kuramoto 3-18-15, Tokushima 770-8503, Japan. Tel.: +81 88 633 9483; Fax: +81 88 633 9484; E-mail: hinoue@genome.tokushima-u.ac.jp

Present address: T. Mukai, Department of Paediatrics, Asahikawa Kosei General Hospital, Asahikawa, Japan.

Present address: Y. Ito, Department of Basic Sciences, Japanese Red Cross Hokkaido College of Nursing, Kitami, Japan .

Introduction

POU1F1/PIT-1, a member of the POU family of transcription factors, is essential for pituitary growth and development.[1–3] POU1F1 also regulates cell-specific gene expression of somatotropes, lactotropes and thyrotropes, and is thus responsible for restricted expression of the corresponding pituitary hormones, GH, PRL and TSH. Previous studies have shown that the promoters of these genes contain a number of POU1F1-binding sites.[2] However, because POU1F1 is present in all three cell types, interactions with other transcription factors [e.g. oestrogen receptor (ER), thyroid hormone receptor (TR), Zn-15, Ets-1, GATA-2, Oct-1 and POU1F1 itself], as well as with transcriptional cofactors [e.g. cAMP-response element–binding protein–binding protein (CBP) and nuclear receptor corepressor (NcoR)], are vital to achieving their selective and targeted expressions.[2,4]

The predominant isoform of POU1F1, POU1F1-α/PIT-1α, is a 291-amino acid (aa) protein containing three important functional motifs: (i) an amino-terminal transactivation domain (TAD; spanning 8–80 aa of the human protein), (ii) a POU-specific domain (POU-S, 128–198 aa) that is unique to this class of transcription factors, and (iii) a carboxy-terminal POU homeodomain (POU-HD, 214–273 aa).[1,5,6] Previous studies suggested that TAD can be further divided into two subregions, R1 (8–45 aa) and R2 (46–80 aa), each encoded mainly by exons 1 and 2, respectively. Functional mapping demonstrated TAD-R1 to be responsible for basal transcriptional activity, whereas TAD-R2 consists of the strong activation region (50–70 aa) as well as the inhibitory/Ras-responsive region (70–80 aa) that is also implicated in interactions with other transcriptional corepressors and coactivators (e.g. ER and TR).[7,8]

Both POU-S and POU-HD contain helix-turn-helix DNA-recognition motifs, and they together constitute a bipartite DNA-binding structure essential for site-specific, high-affinity DNA binding of POU1F1 as well as for its dimer formation and specific protein–protein interactions.

In mammals, including humans, two minor POU1F1 isoforms, POU1F1-β/PIT-1β and PIT-1T, have been identified.[9–12] Both are generated by the alternative use of the splice acceptor site for exon 2, and thus, as compared to POU1F1-α, they only differ by additional aa residues (26 and 14 aa, for POU1F1-β and PIT-1T, respectively) inserted between the R1 and R2 subregions. Nevertheless, POU1F1-β and PIT-1T have been described as exhibiting different expression patterns and unique transcriptional properties. As opposed to POU1F1-α, POU1F1-β suppresses *GH*, *PRL* and *TSHβ* promoters in a pituitary-specific manner, blocking Ras-induced *PRL* promoter activity, whereas PIT-1T appears to be a thyrotrope-specific isoform required for optimal *TSHβ* promoter activation.

In murine models, a point mutation (p.W261C) or a genetic rearrangement (Pit-1^{dwj}) in the *Pou1f1* gene results in dwarfism and anterior pituitary hypoplasia with Gh, Prl and Tsh deficiencies.[13,14] In humans, a number of *POU1F1* mutations have been described in a subset of patients with combined pituitary hormone deficiency (CPHD; MIM 613038).[3,4] In CPHD patients with *POU1F1* mutations, deficiencies of GH and PRL are generally complete and present early in life, whereas TSH deficiency can be more variable. The production of ACTH, LH and FSH is preserved. Brain magnetic resonance imaging (MRI) may show a normal or hypoplastic anterior pituitary. The majority of *POU1F1* mutations identified to date show recessive inheritance; however, at least six (p.P14L, p.P24L, p.Q167K, p.K216E and p.R271W) are reportedly inherited in a dominant manner with highly variable penetrance. Of these, p.R271W is the most frequent, having been identified in different ethnic groups. It has been suggested that the p.R271W form of POU1F1 may impair dimerization and act as a dominant-negative inhibitor of the wild-type POU1F1.[15]

In the present study, we describe the identification and characterization of a novel splice site mutation (Ex2 + 1G>T) of the *POU1F1* gene, which is found in a heterozygous state in Japanese identical twin brothers presenting an exceptionally mild CPHD phenotype. The mutation most likely leads to skipping of exon 2, and generation of a mutant protein, POU1F1 Δ48-72, which merely lacks most of the TAD-R2 subregion. *In vitro* functional study of the mutated protein showed only modest reductions in its transactivation activity in nonpituitary cells, while potentially acting in a dominant-negative manner on the endogenous activity of POU1F1 in pituitary cells.

Subjects and methods

Patients

This study was approved by the Ethics Committee for Human Genome/Gene Research at the University of Tokushima. Patients were recruited as part of the study of the Japan Growth Genome Consortium for genetic analysis of Japanese families with hereditary short stature.[16,17] After obtaining written informed consent, genomic DNA was extracted from peripheral blood leucocytes. DNA from 188 unrelated healthy Japanese subjects (94 women and 94 men) was used for mutation controls.

DNA analysis

The six *POU1F1*-coding exons and their flanking intronic regions, as well as the putative promoter, were analysed by sequencing. Primer sequences are shown in Table S1-1 and 2. PCR and sequencing reactions were performed as described previously.[16,17] The frequency of the Ex2 + 1G>T mutation in control subjects was determined using a mismatched-primer PCR-RFLP assay. PCR was carried out using primers hPOU1F1_F2NF (Table S1-1) and hPOU1F1_Int2_RFLP_R1: 5′-TCCCCAAATTCAATAACATG-TAAAAGACAACTTTggTTA-3′ (lower-case letters indicate the mismatched bases). Digestion of the wild-type allele with *Bst*EII (NEB, Beverly, MA, USA) yielded two fragments (268 and 40 bps), whereas the mutant allele was identified by the presence of undigested fragments (308 bp).

Cell cultures

HEK293T and COS-7 cells were maintained in DMEM (Invitrogen, Tokyo, Japan) supplemented with 10% foetal bovine serum (FBS) and antibiotics. Rat GH3 cells were grown in DMEM/F12 (Invitrogen) supplemented with 10% horse serum, 2·5% FBS and antibiotics.

Heterologous splicing assay

The *POU1F1* exon 2 and its flanking intronic sequence (675 bp) were amplified by PCR from the DNA of an affected individual and a control subject (Table S1-3), subcloned into the pSPL3 vector (Invitrogen), and designated as pSPL3-POU1F1-Ex2-WT or pSPL3-POU1F1-Ex2-MUT. Splicing assays were performed in HEK293T or COS-7 cells (1×10^6 cells/6-cm dish), which were transfected with 8 μg of plasmid DNA using FuGENE HD (Roche, Indianapolis, IN, USA). Forty-eight hours later, total RNA was isolated using an RNeasy Mini kit (Qiagen, Valencia, CA, USA) and reverse-transcribed using Superscript III (Invitrogen). Spliced products were detected by PCR with the primer combination SD6 and SA2 (vector-specific set), or exon 2-specific F1/F2 and SA2 (Table S1-4). Amplification of *β-actin* mRNA was used to assess reaction efficiency.

Expression and promoter–reporter constructs

A wild-type human POU1F1 expression vector, POU1F1-WT-pcDNA3, was provided by Dr Y. Okimura (Kobe Women's University). An in-frame deletion of exon 2 was incorporated into the POU1F1-WT-pcDNA3 using a KOD-Plus-Mutagenesis kit (Toyobo, Osaka, Japan) and designated as POU1F1-Δ48-72-pcDNA3. Full-length p300 and CBP expression vectors were gifts from Dr S. Ishii (RIKEN). Luciferase reporter constructs, rPRL0.6-Luc-pGL3 and rGH0.6-Luc-pGL3, containing either the rat *Prl* (−484 to +16664 relative to the transcription start site) or the rat *Gh* (−555

to +64) promoter sequence, were created by PCR amplification of the corresponding regions and subcloning into a pGL3-Basic plasmid (Promega, Madison, WI, USA). Oligonucleotide sequences used are shown in Table S1-5 and 6.

Immunoblotting

Western blotting of whole-cell lysates from GH3 or transfected HEK293T cells was carried out according to the standard procedure. Subcellular fractionation of transfected cells was performed using the NE-PER kit (Pierce, Rockford, IL, USA). The following primary antibodies were used: anti-PIT-1 (1:1000 dilution; SCB, Santa Cruz, CA, USA), anti-p62 (1:2000; BD Biosciences, San Jose, CA, USA), anti-PARP (1:1000; CST, Tokyo, Japan), anti-GAPDH (1:4000; Clontech-Takara, Kyoto, Japan) and anti-Actin (1:5000; Sigma, St. Louis, MO, USA) antibodies.

Indirect immunofluorescence

Immunofluorescence staining of transfected HEK293T cells was performed as described previously,[16] using anti-PIT-1 antibody (1:100) and Alexa Fluor 546-conjugated goat anti-rabbit IgG (1:200; Invitrogen) as the primary and secondary antibodies, respectively.

Luciferase reporter gene assay

HEK293T cells were seeded on collagen-coated 24-well plates (Iwaki, Nagoya, Japan) 1 day before transfection (5×10^4 cells/well), after which the reporters (pGL3 250 ng, pRL-TK 12·5 ng) and POU1F1-WT or Δ48-72 expression plasmid (250 ng) were introduced into cells at a 3:1 ratio of FuGENE HD (μl) to DNA (μg). Forty-eight hours after transfection, the cells were lysed and analysed for luciferase activity using a Dual-Luciferase Reporter Assay System (Promega). To improve efficiency in GH3 cells, which are refractory to transient transfection, these cells (1×10^5 cells/well) were transfected in suspension immediately after trypsinization at a 5:1 ratio of FuGENE HD to DNA, and the assay was performed 72 h later.

Electrophoretic mobility shift assay

Electrophoretic mobility shift assay (EMSAs) were performed using nuclear extracts from GH3 or transfected HEK293T cells, as described previously.[17] The unlabelled and biotin-labelled human hGHRHR-P2 probes (the sense sequence, 5′-ATCCTGGTGAATATTCAGCGGTCT-3′) and those derived from the rat *Prl* P3 promoter sequence[18] (rPRL-P3; Panomics, Redwood City, CA, USA) were utilized.

Statistical analysis

Data are presented as means ± SD. Statistical significance was analysed employing the two-tailed unpaired *t*-test for comparisons between control and experimental groups. $P < 0{\cdot}05$ was considered statistically significant.

Results

Case report

In September 1993, 5-year-old identical twin brothers (Family F: II.1 and II.2; Fig. 1a) were referred to the paediatric endocrinology clinic of the Asahikawa Medical University Hospital to determine the aetiology of their short stature. They were the first children of unrelated Japanese parents, born by caesarean section on the first day of the 38th week of gestation. Both parents were healthy, and

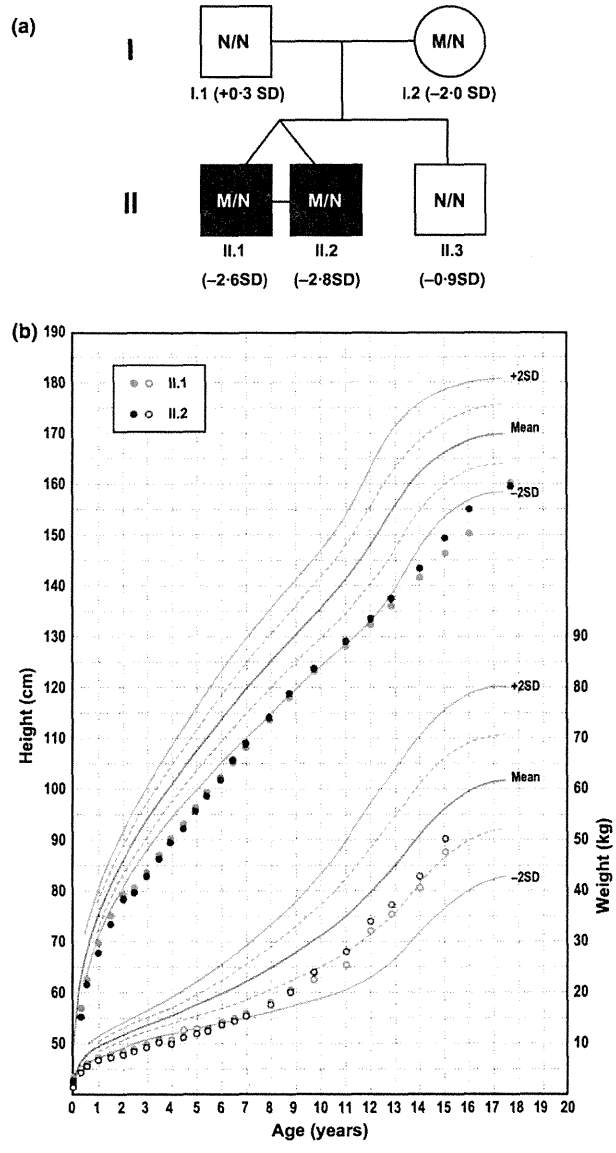

Fig. 1 Pedigree of Family F. (a) Pedigree of Family F with the *POU1F1* Ex2 + 1G>T mutation. Black filled symbols identify index cases. Males, squares; females, circles; M, mutated allele; N, normal allele. (b) Growth curves of patients II.1 and II.2. Heights and body weights are plotted on the Cross-Sectional Growth Chart 1990[30] for Japanese boys (0–18 years old). Closed and open circles (red, II.1; green, II.2) indicate the height and weight of the patients, respectively.

the father had a normal adult height (I.1: 37 years old, 172·1 cm/+0·3 SD), whereas the mother was rather small in stature (I.2: 38 years old, 148·0 cm/−2·0 SD). At birth, the patients were found to be small for gestational age (birth length and weight of II.1: 44·6 cm/−2·3 SD and 2364 g/−1·8 SD and II.2: 43·0 cm/−3·1 SD and 1942 g/−2·9 SD). They had episodes of transient neonatal hypoglycaemia and hyperbilirubinaemia. The mother had no medical history of hypothyroidism. After delivery, she had breastfed both infants without problems, but soon switched to formula feeding because she developed post-transfusion hepatitis. At the first hospital visit, the patient's heights were more than 2·5 SD below the average for boys of their age, and bone ages were delayed more than 2 years behind chronological age (Table 1). Results of hormonal evaluation indicated that they had partial GH deficiency, showing blunted GH peak responses (<6 ng/ml) to at least two different stimuli but more than 3 ng/ml to all stimuli on the GH provocative tests, together with decreased serum IGF-I levels. Their serum IGFBP-3 levels were not measured. Basal and TRH-stimulated levels of PRL were low in both brothers. Basal free T4 and TSH levels were within normal range, and the peak TSH responses after TRH stimulation were normal or slightly blunted. Their serum LH and FSH levels were in the prepubertal range both before and after LHRH stimulation. Neither basal nor stimulated levels of ACTH and cortisol were measured. No brain MRI data were obtained for either patient. Based on the clinical and endocrinological findings, they were diagnosed as having partial CPHD, with mild GH and PRL deficiencies and borderline TSH deficiency. They had no or only mild symptoms. Eventually, it was decided that medical therapy, including GH and levothyroxine administration, was not necessary. The constructed growth chart showed similar growth curves for the brothers throughout the entire period of growth and indicated lack of a pubertal growth spurt (Fig. 1b). Their final heights were II.1: 160·4 cm/−1·8 SD and II.2: 159·8 cm/−1·9 SD. A younger brother's height was within normal range (II.3: 135·8 cm/−1·5 SD at age 11 years). In May 2011, the 56-year-old mother agreed to donate blood samples. Her laboratory tests yielded the following results: basal GH 0·07 ng/ml [reference range (RR) 0·28–1·64], IGF-I 89 ng/ml (−1·37 SD; RR 74–208), IGFBP −3 1·76 μg/ml (RR 1·99–3·19), PRL 1·38 ng/ml (RR 6·12–30·5), TSH 1·84 μIU/ml (RR 0·50–5·00), free T3 3·36 pg/ml (RR 2·30–4·30), free T4 1·08 ng/ml (RR 0·90–1·70), cortisol 9·0 μg/ml (RR 4·0–18·3) and ACTH 9·8 pg/ml (RR 7·2–63·3). Thus, her data were at least suggestive of mild GH and PRL deficiencies, similar to the clinical presentations of her affected sons, but a definitive diagnosis could not be established owing to lack of GH secretion data and brain MRI.

A novel Ex2 + 1G>T mutation in the POU1F1 gene affects splicing of exon 2

In both affected brothers of Family F, a heterozygous Ex2 + 1G>T (c.214 + 1G>T) mutation of *POU1F1* was identified (Fig. 2a). This nucleotide change disrupted a highly conserved GT dinucleotide sequence of the splice donor site at the exon 2–intron 2 boundary. The Ex2 + 1G>T mutation was also heterozygous in their mother (I.2; Fig. 2b), but was not found in the father or a younger brother, or in any of the 188 Japanese controls.

The effect of Ex2 + 1G>T on *in vitro* splicing efficiency was examined using minigene constructs, POU1F1-Ex2-WT and Ex2-MUT (Fig. 2c). When transfected into HEK293T cells, subsequent RT-PCR analysis using vector-derived primers SD6 and SA2 showed that POU1F1-Ex2-WT produced two splice products (Fig. 2d, top panel): a prominent 332-bp band reflecting exon 2 inclusion and a very faint 410-bp product resulting from alternative use of the exon 2 splice acceptor site (i.e. *POU1F1-β* isoform). On the other hand, POU1F1-Ex2-MUT generated only one product that did not contain exon 2. When using SA2 and *POU1F1*-specific primers (F1 and F2), a clear single band corresponding to the normally spliced products (F2 × SA2) as well as a faint band representing the *POU1F1-β* isoform (F1 × SA2) were observed for POU1F1-Ex2-WT, but these were not detected for Ex2-MUT (Fig. 2d, middle panels). Similar observations were also made after transfecting COS-7 cells (data not shown). Thus, our data suggested that Ex2 + 1G>T results in a large decrease in splicing efficiency

Table 1. Clinical and hormone data at initial presentation

									GH peak (ng/ml)	TSH (μIU/ml)	PRL (ng/ml)	LH (mIU/ml)	FSH (mIU/ml)
Subject	Sex	Age (years)	Height (cm)	Weight (kg)	BA (years)	Free T4 (ng/dl)	IGF-1 (ng/ml)	T (ng/dl)	Arg; Ins; L-dopa; GHRH	Baseline; under TRH	Baseline; under TRH	Baseline; under LHRH	Baseline; under LHRH
II.1	M	5·5	98·7 (−2·6 SD)	13·1 (−1·9 SD)	3·4	1·67	20	<5	5·04; 3·90; 6·64; 9·47	1·23; 12·5	0·95; 4·77	0·23; 4·02	1·40; 6·32
II.2	M	5·5	97·9 (−2·8 SD)	12·9 (−2·0 SD)	3·2	1·60	20	<5	8·34; 4·76; 4·67; 12·7	1·35; 14·4	0·94; 6·00	0·26; 3·87	1·94; 6·24
II.3	M	1·1	73·0 (−0·9 SD)	n/a	n/a	n/a	n/a	n/a	n/a	n/a	n/a	n/a	n/a

BA, bone age using the radius–ulna–short bones (RUS) method; T, testosterone; Arg, arginine; Ins, insulin; n/a, not available. Serum GH concentrations were measured using an IRMA kit (Daiichi Radioisotope Laboratories, Tokyo, Japan), and the original GH values (II.1, 8·07; 6·25; 10·6; 15·1; II.2, 13·3; 7·62; 7·48; 20·3) were corrected using the formula recommended by the Foundation for Growth Science in Japan to obtain the approximate values based on the International Standard of recombinant human GH. Reference values for age are as follows: free T4, 1·1–2·6; IGF-1, 29–173; testosterone, <10; GH peak, >6 (arginine, insulin, L-dopa and GHRH); TSH, 0·3–3·5 (baseline), 15–35 (under TRH); PRL, 1·7–15·4 (baseline), 29·4–35·8 (under TRH); LH, 0·2–1·2 (baseline); FSH 1·4–3·0 (baseline).

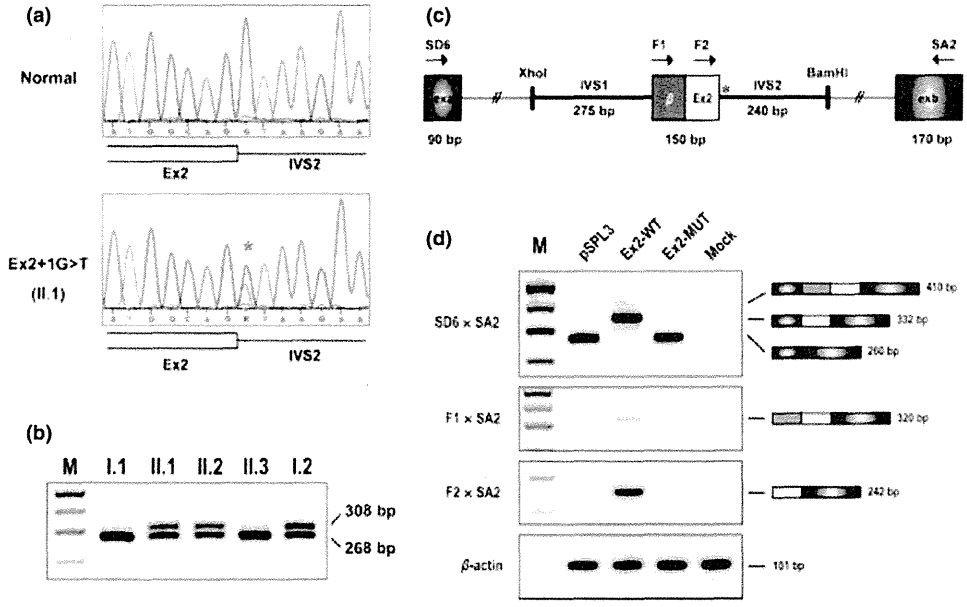

Fig. 2 A novel heterozygous Ex2 + 1 G>T splicing mutation in the *POU1F1* gene. (a) Sequence chromatograms display a portion of the exon 2–intron 2 boundary from a control individual (upper panel) and the index patient in Family F (II.1, lower panel). Patient F: II.1 has a heterozygous G>T transition (red asterisk) at position 1 of intron 2 (Ex2 + 1G>T), which abolishes the canonical donor splice site (GT dinucleotides). Ex, exon; IVS, intervening sequence. (b) In a mismatch PCR-RFLP assay, digestion of a 308-bp amplicon with BstEII yields 268- and 40-bp fragments (the 40-bp fragment is too short to be visible on the agarose gel). This mutation abolishes the BstEII site, and the 308-bp fragment remains intact (II.1, II.2 and I.2). Shown is a black/white inverted image of a gel stained with ethidium bromide. M, DNA size marker. (c) Representation of the pSPL3-POU1F1-Ex2-WT (wild-type) or Ex2-MUT (mutant) minigene constructs. A genomic fragment, containing *POU1F1* exon 2 (150 bp) and 275 bp of the 5′- and 240 bp of the 3′-intronic flanking sequence, was subcloned into the XhoI/BamHI site of pSPL3. Open box, exon 2 of *POU1F1*; grey box, an extended exon 2β specific for the POU1F1-β isoform; shaded boxes, pSPL3 vector exons, exa and exb; horizontal arrows, vector-derived primers SD6 and SA2, and exon 2-specific primers, F1 and F2. Note that primer F1 is specific to the *POU1F1-β* isoform, whereas F2 is common to both the α and the β isoform. Mutation site is indicated by an asterisk. (d) *In vitro* splicing assay. HEK293T cells were transiently transfected with POU1F1-Ex2 minigene constructs or empty pSPL3 vector (negative control). Subsequent RT-PCR analysis was performed with four different sets of primers. Top panel, amplicons obtained with the primer pair SD6/SA2. Note that the Ex2-WT construct yielded two bands of 332 and 410 bps that correspond to the inclusion of exons 2 and 2β respectively, while only a 260-bp band was generated by the Ex2-MUT or empty vectors. Middle panels, the primer pairs F1/SA2 or F2/SA2 produced the normally spliced products from the Ex2-WT construct, but no band is seen in the Ex2-MUT construct. Lower panel, RT-PCR products for β-actin (a RT-PCR quality control) are shown. Black/white inverted images are shown.

and in skipping of exon 2, rather than in the activation of a cryptic donor splice site.

POU1F1-Δ48-72 construct does not affect nuclear targeting and DNA binding in HEK293T cells

As our *in vitro* splicing assay results indicated that Ex2 + 1G>T causes an in-frame skipping of this exon, we generated a mutant expression construct with deletion of exon 2 (POU1F1-Δ48-72), and its functional properties were compared with those of the wild-type construct (POU1F1-WT). Immunoblotting of total cell lysates from POU1F1-WT-transfected HEK293T cells with a POU1F1-specific antibody revealed 33- and 31-kDa immunoreactive bands, arising from alternative translation initiation codon usage of *POU1F1* mRNA,[19] at levels similar to endogenous proteins in GH3 cells (Fig. S1). On the other hand, two smaller bands, 30 and 28 kDa, corresponding to forms with exon 2 deletion, were detected in cells transfected with POU1F1-Δ48-72.

We next examined whether Δ48-72 affects nuclear localization of POU1F1. Subcellular fractionation of POU1F1-WT or Δ48-72-expressing HEK293T cells followed by immunoblotting showed strong nuclear localization in each case (Fig. 3a). Consistently, immunocytochemical staining for POU1F1 showed virtually identical, intense nuclear staining for both WT and Δ48-72 forms (Fig. 3b).

We further performed EMSAs using two different EMSA probes containing previously characterized POU1F1-binding sites, one specific for the distal P2-binding element of the human *GHRHR* promoter (hGHRHR-P2)[17] and the other from the rat *Prl* proximal 3P region (rPRL-P3).[18] Nuclear extracts from POU1F1-WT-expressing cells formed a distinct DNA–protein complex in both cases (Fig. 3c), which was confirmed by supershift with anti-POU1F1 antibody. Similar EMSA results were obtained in nuclear extracts from the POU1F1-Δ48-72-expressing cells, suggesting DNA-binding activity to be unaffected by the mutation.

POU1F1-Δ48-72 exhibits reduced but not abolished transactivation capacity and an impaired synergic interaction with p300 in HEK293T cells

To characterize the effect of Δ48-72 on the function of POU1F1 in transactivation of target promoters, HEK293T cells were

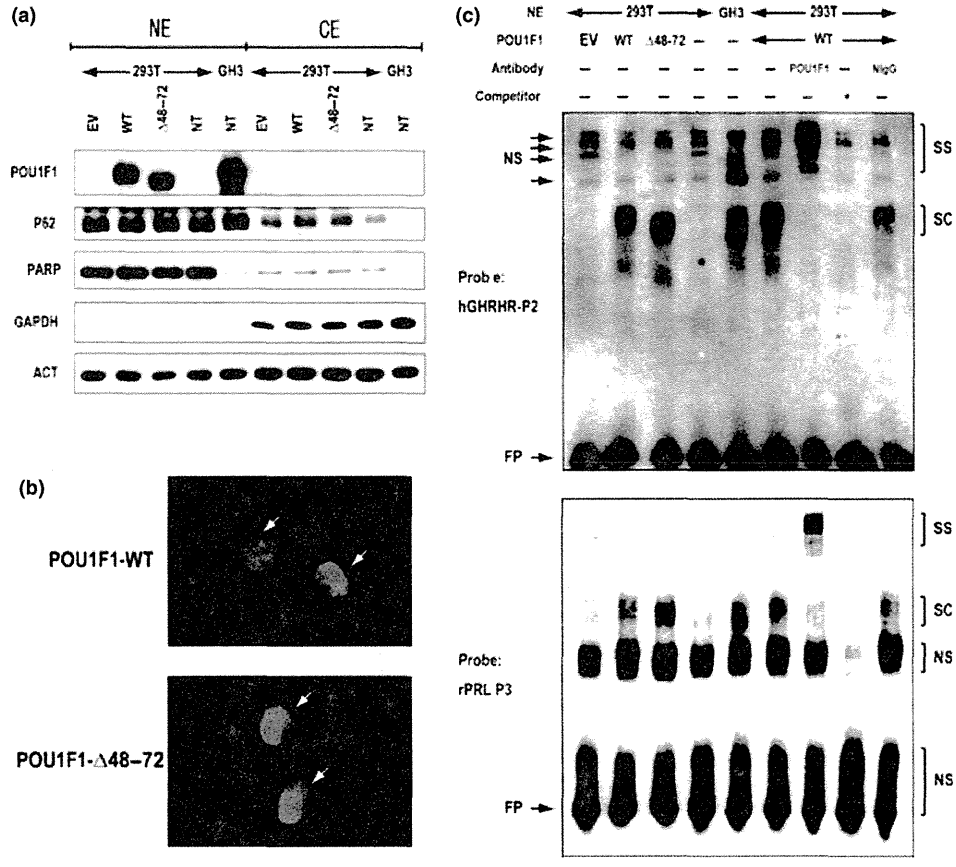

Fig. 3 The Δ48-72 mutant POU1F1 maintains normal nuclear targeting and DNA-binding ability. (a) HEK293T cells were transfected with wild-type (WT) or Δ48-72 mutant POU1F1, or empty vector (EV), and subjected to subcellular fractionation as described in Subjects and methods. As a control, the same procedures were carried out simultaneously with nontransfected (NT) 293T and GH3 cells. Equal amount of protein from either the nuclear (NE; 1 μg per lane) or the cytoplasmic (CE; 10 μg per lane) fractions were loaded on a 10–15% SDS-PAGE gel, transferred and reacted with anti-POU1F1 antibody. To assess the purity of the NE and CE fractions, immunoblot analysis was also conducted with antibodies against nuclear (p62 and PARP) and cytoplasmic (GAPDH) marker proteins. Actin (present in both NE and CE fractions) was probed as a loading control. (b) Indirect immunofluorescent localization of POU1F1 in HEK293T cells transiently transfected with POU1F1-WT (upper) or Δ48-72 (lower) expression constructs. Merged images of anti-POU1F1 (red) and DAPI (blue) are shown. White arrows indicate a nucleus positive for POU1F1, which appears pink as the red stain is overlaid with blue. (c) Electrophoretic mobility shift assays (EMSAs). Nuclear extracts (NE) from transfected HEK293T and GH3 (positive control) cells were prepared and subjected to EMSA with POU1F1-specific oligonucleotide probes (hGHRHR-P2 and rPRL-P3). Competition experiments were performed with unlabelled competitor probes at a 100-fold molar excess. For supershift experiments, antibodies specific for POU1F1 or normal IgG (NIgG; as a negative control) were used. SC indicates POU1F1-specific complex; SS, supershifted complex; NS, nonspecific bands and complex; FP, free probe.

cotransfected with various amounts of either POU1F1-WT or Δ48-72 expression constructs with luciferase reporter genes containing rat *Prl* or *Gh* proximal promoter sequences (rPRL0.6-Luc or rGH0.6-Luc). As shown in Fig. 4a, POU1F1-Δ48-72 showed significantly decreased, but not absent, transcriptional activity (61–81% to the WT activities). When cotransfected with WT, equivalent amounts of Δ48-72 did not inhibit instead additively activated rPRL0.6-Luc and rGH0.6-Luc activities (Fig. 4b), suggesting that Δ48-72 does not exhibit a dominant-negative effect in HEK293T cells.

CBP and p300 were previously described to act as coactivators of a large number of transcription factors, including POU1F1.[20] Consistently, cotransfection of the POU1F1-WT with either the CBP or p300 expression constructs resulted in a synergistic enhancement of transactivation of the rat *Prl* and *Gh* promoters (Fig. 4c). When POU1F1-Δ48-72 was cotransfected with CBP, a similar synergy was observed, whereas no such effects were seen with p300, suggesting the Δ48-72 mutant to be specifically defective in its ability to synergize with p300.

POU1F1-Δ48-72 displays a dominant-negative activity against endogenous POU1F1 and suppresses the rat Gh promoter activity in GH3 cells

Because previous studies suggested the possible cell type specificity of dominant-negative effects of some POU1F1 mutations, we sought to examine the effect of the Δ48-72 mutation against endogenous POU1F1 protein. For this purpose, we conducted reporter assays using GH3 somatolactotrope cells, which express *Pou1f1* as well as *Prl* and *Gh* genes. As shown in Fig. 5, the baseline reporter

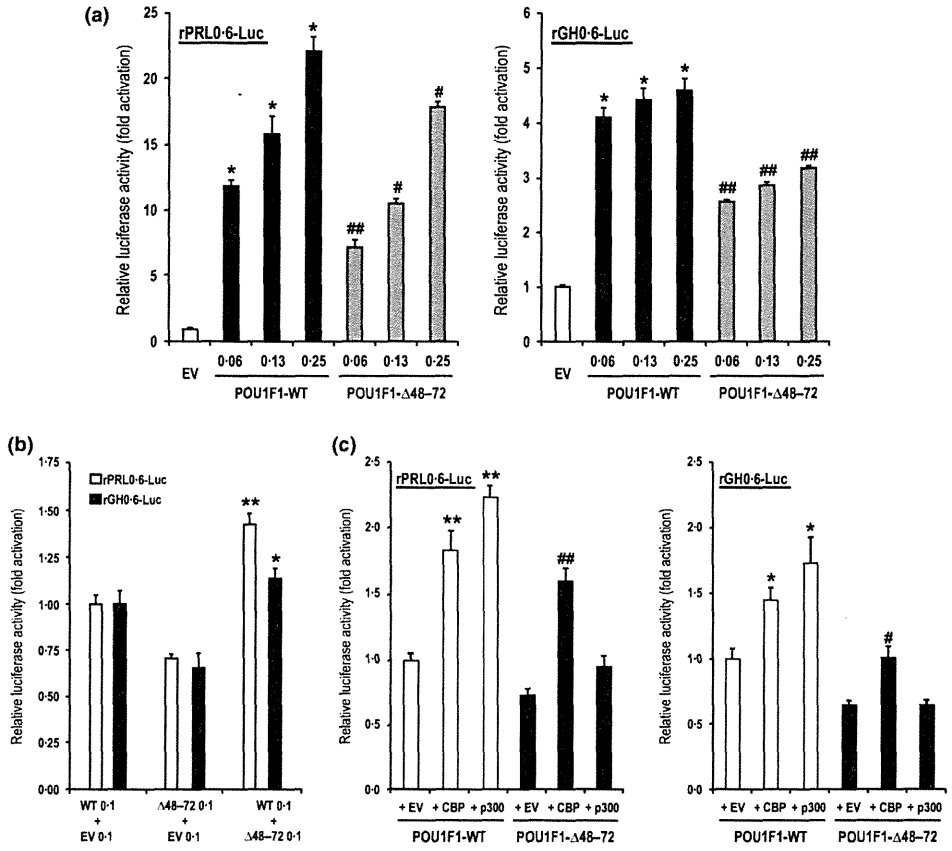

Fig. 4 Reduced transactivation ability and impaired synergy with p300 of the Δ48-72 POU1F1 form. A. HEK293T cells seeded in a 24-well plate were cotransfected with a reporter construct (rPRL0.6-Luc, left; rGH0.6-Luc, right panel), a renilla luciferase construct (pRL-TK, for normalization) and increasing amounts (0·06–0·25 μg DNA per well) of plasmid encoding wild-type (WT) or Δ48-72 mutant human POU1F1. Total amounts of transfected DNA were kept constant by adding empty vector pcDNA3 (EV) as appropriate. The cells were lysed 48 h after transfection, and luciferase activity was measured. Data were normalized and expressed as fold activation relative to the value of the 'EV only' control, which was set to 1. White bar, EV; black bars, POU1F1-WT; dark grey bars, POU1F1-Δ48-72. Each bar represents the mean ± SD of four determinations in one representative series of experiments out of three performed. The statistical significance of differences was determined using the two-tailed unpaired *t*-test. $^{*}P < 0.0001$ *vs* EV, $^{\#}P < 0.001$ and $^{\#\#}P < 0.0001$ *vs* POU1F1-WT. (b) To assess whether the Δ48-72 mutant can inhibit the ability of the WT protein to transactivate the *GH* and *PRL* promoters, equal amounts (0·1 μg each per well of a 24-well plate) of POU1F1-WT and Δ48-72 plasmid DNAs were transfected into HEK293T cells along with either rPRL0.6-Luc or rGH0.6-Luc reporter plasmid, and luciferase assays were carried out. Cells transfected with POU1F1-WT or Δ48-72 alone, keeping the amount of DNA constant by addition of empty vector (EV), were compared. Data were normalized and expressed as fold activation relative to the values of the 'WT+EV' control, which were set to 1. White bar, rPRL0.6-Luc; black bars, rGH0.6-Luc. One representative experiment out of four is shown. $^{*}P < 0.05$ and $^{**}P < 0.0001$ *vs* WT+EV. (c) To evaluate the effects of the Δ48-72 mutation on the synergistic interactions between POU1F1 and either cAMP-response element binding protein–binding protein (CBP) or p300, as coactivators, on *GH* and *PRL* promoters, POU1F1-WT and Δ48-72 were transfected with either CBP or p300 expression constructs as indicated, along with either rPRL0.6-Luc or rGH0.6-Luc. Luciferase assays were then performed. Relative luciferase activity is indicated as the mean ± SD fold activation relative to the value of the 'POU1F1-WT+EV' transfection (set to 1). A representative result from three independent experiments is shown, each performed in quadruplicate and each yielding similar results. $^{*}P < 0.001$ and $^{**}P < 0.0001$ *vs* EV, $^{\#}P < 0.001$ and $^{\#\#}P < 0.0001$ *vs* EV.

gene activities (cotransfected with empty vector) of the rPRL0.6-Luc and rGH0.6-Luc constructs were significantly elevated, reflecting endogenous gene expressions. Consistent with previous observations showing that cotransfection with wild-type POU1F1 elicited only marginal enhancements of target promoter activities in pituitary cells,[11,21] the introduction of POU1F1-WT into GH3 cells showed only small but significant increases in reporter gene activities, with maximum inductions of 1·22- and 1·17-fold for *Prl* and *Gh* promoters, respectively. Unlike with POU1F1-WT, transfection of POU1F1-Δ48-72 significantly suppressed rGH0.6-Luc activity in a dose-dependent manner (53·9% inhibition at the maximum dose), while suppressing rPRL0.6-Luc activity only at the highest dose (84·5% inhibition).

Discussion

The classification and distribution pattern of the disease-associated *POU1F1* mutations showed that the majority (approximately 60%) are missense mutations within the POU-S and POU-HD domains (Fig. S2, Table S2), encoded by exons 4 and 6, respectively. Meanwhile, only a few mutations specifically affecting the TAD region (e.g. p.P14L and p.P24L) have been described to date, and the same

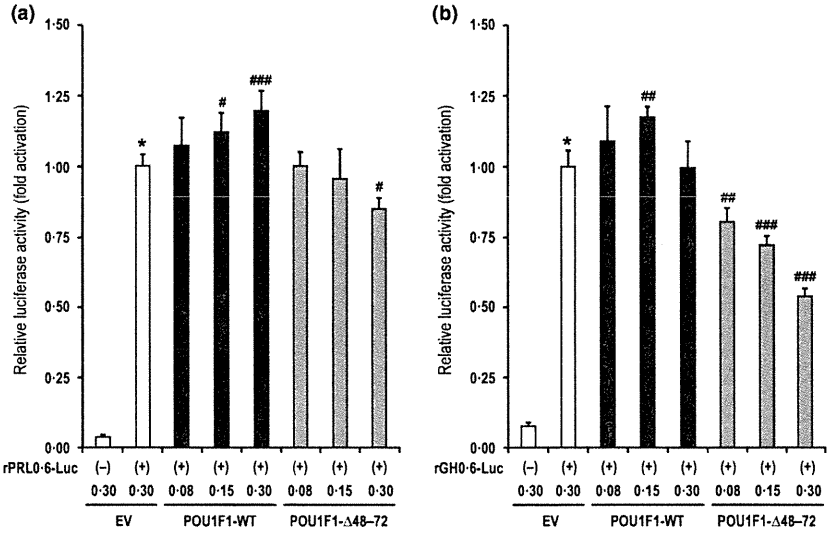

Fig. 5 The Δ48-72 mutant POU1F1 inhibits the activities of the *PRL* and *GH* promoters in GH3 cells. GH3 cells seeded in a 24-well plate were transfected with the rPRL0.6-Luc or rGH0.6-Luc constructs and indicated amounts (μg) of expression vectors encoding POU1F1-WT and POU1F1-Δ48-72, or EV, using an optimized cell-specific protocol (see Subjects and methods). The pRL-TK vector was also used as an internal control, pGL3-Basic as a negative control. Cells were harvested 72 h after transfections, and luciferase activities were measured. Relative luciferase activity is indicated as the mean ± SD fold activation relative to the value of each reporter without POU1F1-WT and POU1F1-Δ48-72 transfections (set to 1). A representative result from three independent experiments is shown, each performed in quadruplicate and each yielding similar results. The statistical significance of differences was determined using the two-tailed unpaired *t*-test. $^{*}P < 0{\cdot}0001$ *vs* empty pGL3-Basic (–), $^{\#}P < 0{\cdot}01$, $^{\#\#}P < 0{\cdot}001$ and $^{\#\#\#}P < 0{\cdot}0001$ *vs* EV.

is true for those involving specific splice sites. To our knowledge, Ex2 + 1G>T is the first demonstration of a mutation specifically involving exon 2, thus affecting TAD, and one of the few examples of aberrant splicing mutations of *POU1F1*.

The *in vitro* splicing assay suggested that Ex2 + 1G>T causes an in-frame skipping of exon 2 in the mRNA, thus generating an internally deleted protein, lacking nearly four-fifths (aa 48–72) of the TAD-R2 subdomain. Functional analysis of POU1F1-Δ48-72 showed reduced but not abolished ability to transactivate the rat *Prl* and *Gh* promoters, with an impaired synergistic interaction with p300, in nonpituitary HEK293T cells. In contrast, dominant-negative activity was exhibited against endogenous POU1F1 in GH3 somatolactotrope cells. These data are generally consistent with previous studies, which suggested the TAD-R2 subregion, as a whole, to play only a contributory role in basal transcriptional activity, although it is likely to be crucial for transcriptional synergy with other transcriptional cofactors (e.g. ER and TR) and, in a similar way, for Ras responsiveness.[7,22–24] A previous report also revealed a motif containing three tyrosine residues separated by six aa residues (Y6Y6Y) encoded by exon 2 to be critical for these effects.[7] In addition, the potential dominant-negative effects of several *POU1F1* mutations have been extensively investigated, and it was emphasized that such effects are largely dependent on experimental conditions and likely to be detectable only in a cell type- or promoter-specific manner.[25,26] The p.R271W mutation was initially found to dominantly inhibit the activation of the *GH* and *PRL* genes by wild-type POU1F1,[27] although this was later disputed.[28] In a more recent study, however, the dominant-negative effects of p.R271W were shown to be detectable only in cells possessing an endogenous POU1F1.[26] In the case of p.K216E, the mutation was found not only to be a superactive stimulator of *GH* and *PRL* promoter activities in nonpituitary CV-1 cells but also to inhibit retinoic acid-induced upregulation of *Pou1f1* expression in GH3 cells.[29]

It should be noted that, in the majority of previously described CPHD patients with *POU1F1* mutations, GH and PRL deficiencies were usually complete, leading to early and progressive growth failure and severe short stature, while the time of onset and the degree of TSH deficiency could be variable. In addition, recessive *POU1F1* mutations reportedly show no obvious phenotype when heterozygous. In this context, our patients had relatively mild short stature and represented a state of partial, rather than an absolute, deficiency of GH. We assume that a similar situation likely occurred in their undiagnosed mother who also presented with mild short stature and harboured the same mutation; however, detailed evaluations including the GH provocative tests and brain MRI are obviously needed before a definitive diagnosis can be established. While a single Ex2 + 1G>T mutation was detected in only one allele of these patients, this mutation falls outside the *POU1F1* mutational hotspot domains, POU-S and POU-HD, and has the potential to act as a dominant-negative inhibitor of endogenous POU1F1. We thus speculate that the rather unusually mild CPHD phenotype of our patients may be attributable to these unique features in mutational location and type of Ex2 + 1G>T. It is also noteworthy that Ex2 + 1G>T is expected to simultaneously disrupt the POU1F1-β and PIT-1T isoforms, containing different 5′-extended variants of exon 2, which are believed to play distinctive and important roles in the regulation of POU1F1-dependent promoters.[11,12] The Ex2 + 1G>T mutation may contribute to the unique clinical phenotypes of our patients in this

regard; however, further experimental evidence is needed to support this hypothesis.

In summary, we have described herein the first identified splice site mutation (Ex2 + 1G>T) at the exon 2–intron 2 splice junction of the *POU1F1* gene, which occurred in heterozygous form in identical twin brothers presenting mild CPHD. The addition of this mutation to the growing list of pathological *POU1F1* mutations may provide meaningful insights into clinical heterogeneity in the expression of individual mutations and a deeper understanding of the structure–function relationships of the POU1F1 protein.

Acknowledgements

We acknowledge the resources provided by the Japan Growth Genome Consortium, and the participating patients and their family members. We would like to thank Professor Yasuhiko Okimura (Kobe Women's University, Kobe, Japan) and Professor Shunsuke Ishii (Tsukuba Life Science Center, RIKEN, Japan) for providing us their expression plasmids. This work was supported by a research grant from Novo Nordisk. This paper is dedicated to Professor Kenji Fujieda who passed away on 19 March 2010 during the completion of this work. Japan Growth Genome Consortium: Department of Paediatrics, Asahikawa Medical College; Department of Endocrinology and Metabolism, National Research Institute for Child Health and Development; Saitama Children's Medical Center; Department of Paediatrics, Hokkaido University Graduate School of Medicine; Department of Paediatrics, Tendo City Hospital; Department of Paediatrics, University of Yamanashi School of Medicine; Department of Paediatrics, Fukui Medical University; Department of Paediatrics, Japanese Red Cross Society Wakayama Medical Center; Department of Paediatrics, Odawara Municipal Hospital; Department of Paediatrics, Graduate School of Medicine, Kyoto University; Department of Paediatrics, Niigata Prefectural Shibata Hospital; Department of Paediatrics, Keio University School of Medicine; Department of Paediatrics, Nagasaki University School of Medicine; Department of Paediatrics, Tottori University Hospital; Department of Paediatrics, Fujieda Municipal General Hospital; Department of Paediatrics, Hiroshima University Hospital; Department of Paediatrics, Kawasaki Municipal Hospital; Department of Paediatrics, Akita Kumiai General Hospital; Igarashi Children's Clinic; Department of Paediatrics, Tokyo Denryoku Hospital; Department of Paediatrics, Hamamatsu University School of Medicine; Department of Paediatrics, Shinsyu University Hospital; Department of Paediatrics, Ehime University Graduate School of Medicine; Institute for Genome Research, The University of Tokushima.

Disclosure

The authors have no conflicts of interest to declare.

References

1 Andersen, B. & Rosenfeld, M.G. (1994) Pit-1 determines cell types during development of the anterior pituitary gland. A model for transcriptional regulation of cell phenotypes in mammalian organogenesis. *The Journal of Biological Chemistry*, **269**, 29335–29338.

2 Andersen, B. & Rosenfeld, M.G. (2001) POU domain factors in the neuroendocrine system: lessons from developmental biology provide insights into human disease. *Endocrine Reviews*, **22**, 2–35.

3 Kelberman, D., Rizzoti, K., Lovell-Badge, R. *et al.* (2009) Genetic regulation of pituitary gland development in human and mouse. *Endocrine Reviews*, **30**, 790–829.

4 Cohen, L.E. & Radovick, S. (2002) Molecular basis of combined pituitary hormone deficiencies. *Endocrine Reviews*, **23**, 431–442.

5 Theill, L.E., Castrillo, J.L., Wu, D. *et al.* (1989) Dissection of functional domains of the pituitary-specific transcription factor GHF-1. *Nature*, **342**, 945–948.

6 Ingraham, H.A., Flynn, S.E., Voss, J.W. *et al.* (1990) The POU-specific domain of Pit-1 is essential for sequence-specific, high affinity DNA binding and DNA-dependent Pit-1-Pit-1 interactions. *Cell*, **61**, 1021–1033.

7 Holloway, J.M., Szeto, D.P., Scully, K.M. *et al.* (1995) Pit-1 binding to specific DNA sites as a monomer or dimer determines gene-specific use of a tyrosine-dependent synergy domain. *Genes & Development*, **9**, 1992–2006.

8 Duval, D.L., Jonsen, M.D., Diamond, S.E. *et al.* (2007) Differential utilization of transcription activation subdomains by distinct coactivators regulates Pit-1 basal and Ras responsiveness. *Molecular Endocrinology*, **21**, 172–185.

9 Theill, L.E., Hattori, K., Lazzaro, D. *et al.* (1992) Differential splicing of the GHF1 primary transcript gives rise to two functionally distinct homeodomain proteins. *The EMBO Journal*, **11**, 2261–2269.

10 Konzak, K.E. & Moore, D.D. (1992) Functional isoforms of Pit-1 generated by alternative messenger RNA splicing. *Molecular Endocrinology*, **6**, 241–247.

11 Jonsen, M.D., Duval, D.L. & Gutierrez-Hartmann, A. (2009) The 26-amino acid beta-motif of the Pit-1beta transcription factor is a dominant and independent repressor domain. *Molecular Endocrinology*, **23**, 1371–1384.

12 Haugen, B.R., Gordon, D.F., Nelson, A.R. *et al.* (1994) The combination of Pit-1 and Pit-1T have a synergistic stimulatory effect on the thyrotropin beta-subunit promoter but not the growth hormone or prolactin promoters. *Molecular Endocrinology*, **8**, 1574–1582.

13 Li, S., Crenshaw, E.B., Rawson, E.J. *et al.* (1990) Dwarf locus mutants lacking three pituitary cell types result from mutations in the POU-domain gene pit-1. *Nature*, **347**, 528–533.

14 Camper, S.A., Saunders, T.L., Katz, R.W. *et al.* (1990) The Pit-1 transcription factor gene is a candidate for the murine Snell dwarf mutation. *Genomics*, **8**, 586–590.

15 Jacobson, E.M., Li, P., Leon-del-Rio, A. *et al.* (1997) Structure of Pit-1 POU domain bound to DNA as a dimer: unexpected arrangement and flexibility. *Genes & Development*, **11**, 198–212.

16 Inoue, H., Kangawa, N., Kinouchi, A. *et al.* (2011) Identification and functional analysis of novel human growth hormone secretagogue receptor (GHSR) gene mutations in Japanese subjects with short stature. *The Journal of Clinical Endocrinology and Metabolism*, **96**, E373–E378.

17 Inoue, H., Kangawa, N., Kinouchi, A. *et al.* (2011) Identification and functional analysis of novel human growth hormone-releasing hormone receptor (GHRHR) gene mutations in Japanese subjects with short stature. *Clinical Endocrinology*, **74**, 223–233.

18 Yan, G.Z., Pan, W.T. & Bancroft, C. (1991) Thyrotropin-releasing hormone action on the prolactin promoter is mediated by the POU protein pit-1. *Molecular Endocrinology*, **5**, 535–541.
19 Voss, J.W., Yao, T.P. & Rosenfeld, M.G. (1991) Alternative translation initiation site usage results in two structurally distinct forms of Pit-1. *The Journal of Biological Chemistry*, **266**, 12832–12835.
20 Cohen, R.N., Brue, T., Naik, K. *et al.* (2006) The role of CBP/p300 interactions and Pit-1 dimerization in the pathophysiological mechanism of combined pituitary hormone deficiency. *The Journal of Clinical Endocrinology and Metabolism*, **91**, 239–247.
21 Ferry, A.L., Locasto, D.M., Meszaros, L.B. *et al.* (2005) Pit-1beta reduces transcription and CREB-binding protein recruitment in a DNA context-dependent manner. *Journal of Endocrinology*, **185**, 173–185.
22 Chang, W., Zhou, W., Theill, L.E. *et al.* (1996) An activation function in Pit-1 required selectively for synergistic transcription. *The Journal of Biological Chemistry*, **271**, 17733–17738.
23 Diamond, S.E., Chiono, M. & Gutierrez-Hartmann, A. (1999) Reconstitution of the protein kinase A response of the rat prolactin promoter: differential effects of distinct Pit-1 isoforms and functional interaction with Oct-1. *Molecular Endocrinology*, **13**, 228–238.
24 Duval, D.L., Jean, A. & Gutierrez-Hartmann, A. (2003) Ras signaling and transcriptional synergy at a flexible Ets-1/Pit-1 composite DNA element is defined by the assembly of selective activation domains. *The Journal of Biological Chemistry*, **278**, 39684–39696.
25 Turton, J.P., Reynaud, R., Mehta, A. *et al.* (2005) Novel mutations within the POU1F1 gene associated with variable combined pituitary hormone deficiency. *The Journal of Clinical Endocrinology and Metabolism*, **90**, 4762–4770.
26 Pellegrini, I., Roche, C., Quentien, M. *et al.* (2006) Involvement of the pituitary-specific transcription factor pit-1 in somatolactotrope cell growth and death: an approach using dominant-negative pit-1 mutants. *Molecular Endocrinology*, **20**, 3212–3227.
27 Radovick, S., Nations, M., Du, Y. *et al.* (1992) A mutation in the POU-homeodomain of Pit-1 responsible for combined pituitary hormone deficiency. *Science*, **257**, 1115–1118.
28 Kishimoto, M., Okimura, Y., Fumoto, M. *et al.* (2003) The R271W mutant form of Pit-1 does not act as a dominant inhibitor of Pit-1 action to activate the promoters of GH and prolactin genes. *European Journal of Endocrinology*, **148**, 619–625.
29 Cohen, L.E., Zanger, K., Brue, T. *et al.* (1999) Defective retinoic acid regulation of the Pit-1 gene enhancer: a novel mechanism of combined pituitary hormone deficiency. *Molecular Endocrinology*, **13**, 476–484.
30 Suwa, S. & Tachibana, K. (1993) Standard growth charts for height and weight of Japanese children from birth to 17 years based on a cross-sectional survey of national data. *Clinical Pediatric Endocrinology*, **2**, 87–97.

Supporting Information

Additional Supporting Information may be found in the online version of this article:

Fig. S1. Western blot analysis.

Fig. S2. Protein domains, genomic organization and pathogenic mutations of POU1F1.

Table S1. Sequence of oligonucleotides used in this study.

Table S2. List of CPHD-associated *POU1F1* mutations reported in the literature.

Please note: Wiley-Blackwell are not responsible for the content or functionality of any supporting materials supplied by the authors. Any queries (other than missing material) should be directed to the corresponding author for the article.

European Journal of Human Genetics (2012) 20, 928–932

www.nature.com/ejhg

EJHG Open

ARTICLE

Relative frequency of underlying genetic causes for the development of UPD(14)pat-like phenotype

Masayo Kagami[1], Fumiko Kato[1], Keiko Matsubara[1], Tomoko Sato[1], Gen Nishimura[2] and Tsutomu Ogata*[,1,3]

Paternal uniparental disomy 14 (UPD(14)pat) results in a unique constellation of clinical features, and a similar phenotypic constellation is also caused by microdeletions involving the *DLK1-MEG3* intergenic differentially methylated region (IG-DMR) and/or the *MEG3*-DMR and by epimutations (hypermethylations) affecting the DMRs. However, relative frequency of such underlying genetic causes remains to be clarified, as well as that of underlying mechanisms of UPD(14)pat, that is, trisomy rescue (TR), gamete complementation (GC), monosomy rescue (MR), and post-fertilization mitotic error (PE). To examine this matter, we sequentially performed methylation analysis, microsatellite analysis, fluorescence *in situ* hybridization, and array-based comparative genomic hybridization in 26 patients with UPD(14)pat-like phenotype. Consequently, we identified UPD(14)pat in 17 patients (65.4%), microdeletions of different patterns in 5 patients (19.2%), and epimutations in 4 patients (15.4%). Furthermore, UPD(14)pat was found to be generated through TR or GC in 5 patients (29.4%), MR or PE in 11 patients (64.7%), and PE in 1 patient (5.9%). Advanced maternal age at childbirth (≥35 years) was predominantly observed in the MR/PE subtype. The results imply that the relative frequency of underlying genetic causes for the development of UPD(14)pat-like phenotype is different from that of other imprinting disorders, and that advanced maternal age at childbirth as a predisposing factor for the generation of nullisomic oocytes through non-disjunction at meiosis 1 may be involved in the development of MR-mediated UPD(14)pat.
European Journal of Human Genetics (2012) **20,** 928–932; doi:10.1038/ejhg.2012.26; published online 22 February 2012

Keywords: genetic cause; maternal age effect; monosomy rescue; UPD(14)pat subtype

INTRODUCTION

Human chromosome 14q32.2 carries a ~1.2 Mb imprinted region with the germline-derived primary *DLK1-MEG3* intergenic differentially methylated region (IG-DMR) and the post-fertilization-derived secondary *MEG3*-DMR, together with multiple imprinted genes.[1,2] Both DMRs are methylated after paternal transmission and unmethylated after maternal transmission in the body, whereas in the placenta the IG-DMR alone remains as a DMR and the *MEG3*-DMR is rather hypomethylated irrespective of the parental origin.[2,3] Furthermore, it has been shown that the unmethylated IG-DMR and *MEG3*-DMR of maternal origin function as the imprinting centers in the placenta and the body, respectively, and that the IG-DMR acts as an upstream regulator for the methylation pattern of the *MEG3*-DMR in the body but not in the placenta.[3]

As a result of the presence of the imprinted region, paternal uniparental disomy 14 (UPD(14)pat) (OMIM #608149) causes a unique constellation of body and placental phenotypes such as characteristic face, bell-shaped small thorax, abdominal wall defect, polyhydramnios, and placentomegaly.[2,4,5] Furthermore, consistent with the essential role of the DMRs in the imprinting regulation, microdeletions and epimutations affecting the IG-DMR or both DMRs of maternal origin result in UPD(14)pat-like phenotype in both the body and the placenta, whereas a microdeletion involving the maternally inherited *MEG3*-DMR alone leads to UPD(14)pat-like phenotype in the body, but not in the placenta.[2,3]

Of the three underlying genetic causes for UPD(14)pat-like phenotype (UPD(14)pat, microdeletions, and epimutations), UPD(14)pat is primarily generated by four mechanisms, that is, trisomy rescue (TR), gamete complementation (GC), monosomy rescue (MR), and post-fertilization mitotic error (PE).[6] TR refers to a condition in which chromosome 14 of maternal origin is lost from a zygote with trisomy 14 formed by fertilization between a disomic sperm and a normal oocyte. GC results from fertilization of a disomic sperm with a nullisomic oocyte. MR refers to a condition in which chromosome 14 of paternal origin is replicated in a zygote with monosomy 14 formed by fertilization between a normal sperm and a nullisomic oocyte. PE is an event after formation of a normal zygote. In this regard, a nullisomic oocyte specific to GC and MR is produced by non-disjunction at meiosis 1 (M1) or meiosis 2 (M2), and non-disjunction at M1 is known to increase with maternal age, probably because of a long-term (10–50 years) meiotic arrest at prophase 1.[7]

However, relative frequency of the genetic causes for UPD(14)pat-like phenotype remains to be determined, as well as that of underlying mechanisms for the generation of UPD(14)pat. Here, we report our data on this matter, and discuss the difference in the relative frequency

[1]Department of Molecular Endocrinology, National Research Institute for Child Health and Development, Tokyo, Japan; [2]Department of Radiology, Tokyo Metropolitan Children's Medical Center, Fuchu, Japan; [3]Department of Pediatrics, Hamamatsu University School of Medicine, Hamamatsu, Japan
*Correspondence: Professor T Ogata, Department of Pediatrics, Hamamatsu University School of Medicine, Hamamatsu 431-3192, Japan. Tel: +81 53 435 2310; Fax: +81 53 435 2312; E-mail: tomogata@hama-med.ac.jp
Received 23 May 2011; revised 10 November 2011; accepted 26 December 2011; published online 22 February 2012